



Convolutional neural networks for accurate identification of mining remains from UAV-derived images

Daniel Fernández-Alonso¹ · Javier Fernández-Lozano² · María Teresa García-Ordás¹

Accepted: 4 November 2023 / Published online: 18 November 2023
© The Author(s) 2023, corrected publication 2023

Abstract

A new deep learning system is proposed for the rapid and accurate identification of anthropogenic elements of the Roman mining infrastructure in NW Iberia, providing a new approach for automatic recognition of different mining elements without the need for human intervention or implicit subjectivity. The recognition of archaeological and other abandoned mining elements provides an optimal test case for decision-making and management in a broad variety of research fields. A new image dataset was created by obtaining UAV images from different anthropic features. A convolutional neural network architecture was implemented, achieving recognition results of close to 95% accuracy. This methodological approach is suitable for the identification and accurate location of ancient mines and hydrologic infrastructure, providing new tools for accurate mapping of mining landforms. Additionally, this novel application of deep learning can be implemented to reduce potential risks caused by abandoned mines, which can cause significant annual human and economic losses worldwide.

Keywords UAV images · Convolutional neural network · Archaeology · Roman mining · Deep learning

1 Introduction and related work

Surveying tasks require important technical and economic resources for the effective and accurate development of research activity and successful implementation of management plans. The use of geographic information systems (GISs) has greatly contributed to simplifying the mapping process in a wide variety of fields (archaeology, [1]; environmental sciences, [2]; engineering, [3]; geology, [4]; risk assessment, [5]). However, the quality of the final product often depends on the expertise and technical skills of the surveyor. In addition, digital image surveying involves a

certain degree of subjectivity depending upon different intrinsic factors, such as image quality, panchromatic hue and resolution. Recent advances in augmented reality (AR) have considerably reduced the human factor, as the interpretation of geospatial data can incorporate a 3D graphical representation of datasets [6–8]. Nevertheless, these techniques only simplify the viewpoint of the surveying feature without providing any information about the morphological expression of the object.

Growing interest in combining GIS and AR methodological approaches has led to the implementation of surveying methods, providing outstanding results in a wide variety of contexts and disciplines. Hence, various research fields, prominently including spatial analysis, archaeology, mining, geology, environmental sciences, civil engineering, and education, have benefited from reliable maps of landforms, features and processes [9–14]. Nonetheless, the potential of these methods still has a reduced impact on the surveying results since the implicit subjective factor of identification and recognition of interesting features remains unaddressed.

For instance, the detection of objects based on images is an important application using deep learning techniques. The precise multistage detection of small objects in target regions [15], while complex, continues to be a challenge in the field of computer vision since the orientations are

✉ María Teresa García-Ordás
mgaro@unileon.es

Daniel Fernández-Alonso
dferna10@estudiantes.unileon.es

Javier Fernández-Lozano
jferl@unileon.es

¹ SECOMUCI Research Groups, Escuela de Ingenierías Industrial e Informática, Universidad de León, Campus de Vegazana s/n C.P., 24071 León, Spain

² Prospecting and Mining Research Area, Higher Technical School of Mining Engineering, University of León, 24071 León, Spain

arbitrary, the scales vary, and the shapes are irregular. Advances in data acquisition technologies, such as the appearance of unmanned aerial vehicles (UAVs), have potentially raised interest in various fields in solving problems that were previously carried out manually [16, 17]. Now, it is possible to capture a large number of high-resolution images that can be rapidly preprocessed and analysed using deep learning techniques [18]. For instance, the identification and description of archaeological and mining patterns makes it possible to simplify the study, identification and mapping of elements of interest in these fields [19–23].

The implementation of methods based on a bidirectional multibranch pyramidal network (BPMFPN) for the detection of objects in real time by UAVs has been demonstrated as robust to scale changes [24–26].

The common use of different models such as Inception-v3, ResNet-50, VGG-16, VGG-19 and Xception to solve problems related to crops and plants [27] reaches a high accuracy of up to 93.82%, suggesting a promising future for this type of work [19, 28–30]. Similar examples in this field have involved the use of a new decision tree (DT) combining texture features (mean and variance) and spectral features (TS-DT) for rice plant detection from UAV images [31]. Many other examples in agriculture have recently been developed [32–34] using UAVs, spectral–spatial techniques and artificial intelligence [35], and these techniques

have also been studied in residential environments by Lin et al. [36].

New advances have been made in the analysis of anthropic features for the identification of linear structures such as roads [37] and other elements by means of automatic detection from blurred images [38] or RGB-D maps [39].

However, in the last few years, the implementation of neuronal networks and UAV images in the mining field has grown [24]. Studies on this topic have also aimed at the identification of defects in rocks [40] and present-day mining areas based on unsupervised classification algorithms [41]. However, until now, no general studies on ancient mining, in particular Roman gold mining, have been developed for automatic detection using UAV images. In this paper, we explore the potential of deep learning to reduce the uncertainties produced during the exploration and mapping of ancient mining landscapes in NW Iberia. A method capable of automating the process of classifying different ancient and recent features has been applied to the identification of Roman gold mining remains. This methodological approach can help archaeologists, geomorphologists, and geologists identify mining patterns such as gold mines and hydraulic infrastructure and is able to differentiate them from other present-day anthropogenic elements such as roads and tracks based upon images captured with UAVs by means of artificial intelligence techniques. In our case, a dataset with old

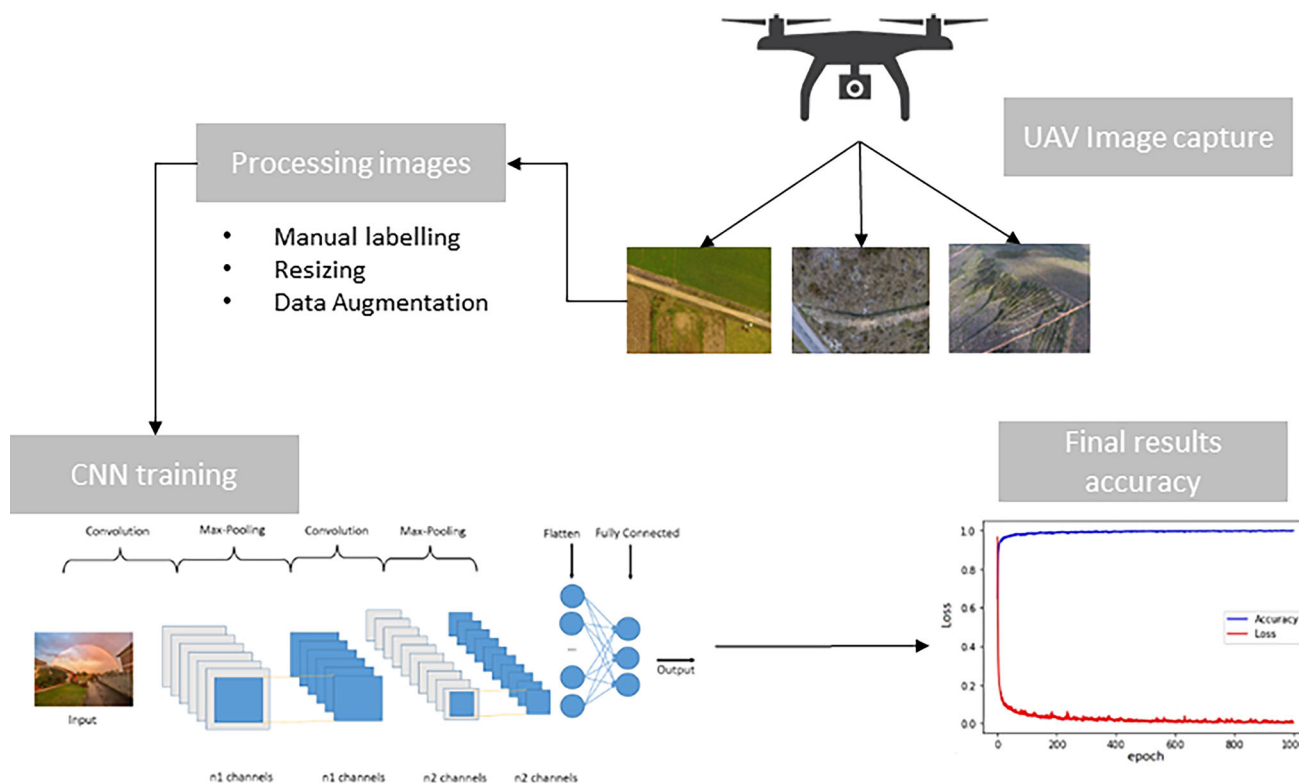


Fig. 1 Summary of the methodology followed in this experiment

mining elements is created, and the main task is to develop an automatic detection method for these elements (crossroads, gold mines, canals).

The proposed model is capable of identifying and recognizing a pattern by alerting the user to the existence of a related pattern. The potential of this methodology relies on the rapid, cost-effective, and accurate surveying of archaeological and mining elements, which will contribute to facilitating the analysis often performed manually by scientists. A graphical abstract with the main steps of this project can be seen in Fig. 1.

Therefore, this paper makes several significant contributions to the field of mining research and cultural heritage preservation. First, we introduce a novel approach for identifying mining remains from UAV-derived images using convolutional neural networks (CNNs). This approach offers several advantages over traditional methods, including the ability to process large regions quickly and accurately, even in areas that are difficult to access. Convolutional neural networks are a type of deep learning neural network algorithm that is particularly well suited for image recognition tasks. They are capable of extracting complex features from images, such as edges, corners, and textures, and can learn to recognize patterns and objects in images with high accuracy, outperforming classical feature descriptors.

Second, we demonstrate the effectiveness of our approach through experiments that show recognition results close to 95% accuracy. Third, we create a new image dataset by obtaining UAV images, which can be used for future research in this field. Finally, we highlight the potential of artificial intelligence in this field and the implications of our work for the protection and study of cultural heritage sites. We believe that our contributions have significant implications for the field of mining research and cultural heritage preservation, and we hope that our paper will inspire further research in this area.

This paper is organized as follows. The research aim of this paper is highlighted in Section 2. An introduction to Roman gold mining infrastructure is presented in Section 3. The methods and materials are detailed in Section 4. In Section 5, the experiments carried out are explained, and the potential of artificial intelligence is supported in Section 6. Finally, Section 7 gives the conclusions.

2 Research aim

The main objective of this work is to automatically identify the remains of ancient Roman mines and ancient water channels, differentiating them from roads and paths using UAV-derived images and deep learning techniques. The advantages provided by this automatic process are mainly the speed of computing large regions, including areas that

are difficult to access, and the greater precision when classifying the elements due to the aerial perspective offered by UAVs. The techniques used correctly label 94.66% of the images evaluated, so they will allow archaeologists, geographers and geologists to improve the identification of new areas of cultural heritage for future study. The main goals of this project are as follows:

- Development of an automatic system for the detection of ancient Roman remains.
- Rapid mass detection capability using UAV imaging.
- Differentiation between Roman canals and dirt roads.
- Analysis of land with difficult road access.

3 Roman gold mining infrastructure in NW Iberia

NW Iberia has one of the largest Roman gold mining complexes in the world, and most of its activity occurred between the 1st and 3rd centuries A.D. Its importance seems to be supported by some relevant Latin authors, such as Pliny the Elder, who wrote about this region (mostly Asturias, Galicia and León), stating that during this period, over 6.5 tons of gold were obtained. The study area is located in the Province of León and comprises an outstanding hydraulic system of channels and water tanks used for exploitation of auriferous materials [42]. The channel infrastructure in this sector exceeds 1,200 km [43]; the longest feature known is over 140 km, and it supplied water to the popular mine of Las Médulas, declared a World Heritage Site in 1997 [44, 45].

Channels were excavated in rock using iron chisels and peaks when brittle (i.e., slate rock), while hard rock was excavated using fire (i.e., quartzite). In general, the channels were built in a standard pattern across their length, assuming average slopes below 1% and widths of 0.3-0.5 m in hard rocks or areas with scarce water resources across the upper exploitation stretches; widths over 1.20-1.50 m in brittle rocks and/or middle exploitation stretches; and widths over 3 m in sedimentary rocks or soils located in the lower sectors of exploitation, also known as leats [43]. Recent works carried out by Andrés Bercianos et al. [46] in the nearby area of Zamora estimated an average flow rate of 0.2-0.4 m³/s considering water depths < 0.35 m. Some of these elements of the hydraulic infrastructure are still recognizable in the landscape, especially in remote mountainous areas that are difficult to access, where no recent anthropic impact due to farming or other human activities is recorded [47].

The channel selected in this study comprises a representative sector of the main hydraulic infrastructure that supplied water to the Las Médulas mine. It is known as the Peña Aguda channel and comprises a nearly 43 km structure with varying widths between 0.9 and 1.20 m across its length.

This channel was excavated in slate rock, which preserves the notches of the chisels on its walls. Water was collected from the Truchillas River, close to the Natural Monument of Truchillas Lake in the La Cabrera Mountains and the nearby Teleno Mountains.

Different mining techniques were implemented to exploit the gold-bearing deposits. Thus, depending upon the geological characteristics (i.e., primary or secondary gold-placer deposits), the extraction technique and exploitation system were modified. This led to a complex infrastructure of mining features that are still recognizable in the landscape. Among the most remarkable structures, according to their geometrical and picturesque morphology, the convergent furrows stand out. This is a system that has been widely developed in areas with reduced slope and material thickness but large size. This system was established in secondary gold-placer deposits broadly represented throughout the northwestern Iberian Peninsula (León, [48]; Zamora, [49]; Salamanca, [47, 50]).

The case study of convergent furrows in Castrocontrigo features one of the most extensive systems of mines, occupying a total extent that exceeds 5 km in length and a surface over 195 ha. It was first studied by Sáenz and Vélez (1974) [51] and was recently explored using LiDAR technology by Fernández-Lozano et al. [48]. Recently, the

implementation of UAVs and visual enhancement techniques allowed Fernández-Lozano and Gutiérrez-Alonso (2016) [52] to improve the identification and description of different mining elements. The Vallico-La Escoba mine, located in the easternmost sector of the Castrocontrigo exploitation site, constitutes an outstanding representative feature of this type of mining infrastructure. Therefore, it can be considered a mining analogue for analysis due to its reduced dimensions (18 ha) and good preservation.

4 Methods and materials

4.1 Dataset

The drone used for this project is a rotary-wing vehicle with 4 engines and vertical take-off. The aircraft was remotely controlled or totally autonomous depending on the different types of flights that were carried out. To obtain the dataset, three flights were carried out, one for each pattern that we aimed to detect in this work. To control these flights, the Pix4DCapture mobile application was used, which allows us to select the parameters that interest us for each flight. As the elements to be recognized are crossroads, Roman water channels and Roman gold exploitations, three flights were



Fig. 2 Patterns with crossroads (top) and without crossroads (bottom)

Fig. 3 Pattern of Roman water channels



carried out with different characteristics that are described below.

4.1.1 Capturing images with a crossroad pattern

This flight was made on November 11, 2020, in the area of Villimer, a village located east of León city. In this case, 2209 images were obtained with and without crossroads. Some images were captured autonomously at 55 and 100 metres of altitude, and others were captured manually at different heights. An example of these image classes can be seen in Fig. 2.

4.1.2 Capturing images with patterns of Roman water channels

The channels are 1.20 metres wide, and on curves, they increase in width to reduce the speed of the water. They have a slope of less than 1%. With these characteristics, the Romans ensured that the water did not have much force when it reached the washing areas, to which it could pull all the mineral sediment.

The flight was carried out on March 8, 2021, in the Corporales area, belonging to the Truchas municipality west of León. In this case, 1646 images were obtained of the water transport channels leading to the Roman mining operations. In this case, it was necessary to sweep up the channels and

capture the images from different perspectives, so manual flight was carried out. Samples of the captured images are shown in Fig. 3.

4.1.3 Capturing images with a Roman gold mining pattern

The Roman gold mining pattern is similar to a broom (see Fig. 4) leading to the location where the Romans refined the material. In the more remote areas, thicker material was used, and where these two areas converged was a washing area where the finest gold could be obtained.

The flight to obtain images of the mine was carried out on March 8, 2021, over the Castrocontrigo mines in León, and 2,082 images were obtained. In this case, manual flights forming circles at a suitable height to capture all the gold mines were carried out.

At the end of this process, a total of 5,892 valid images of size 4000×3000 of the different patterns were obtained to train our model.

4.2 Convolutional neural networks

A convolutional neural network (CNN) is a deep learning neural network algorithm that can take a two-dimensional input, an image and a matrix, and is capable of extracting complex characteristics from the input data.

Fig. 4 Roman gold mining pattern



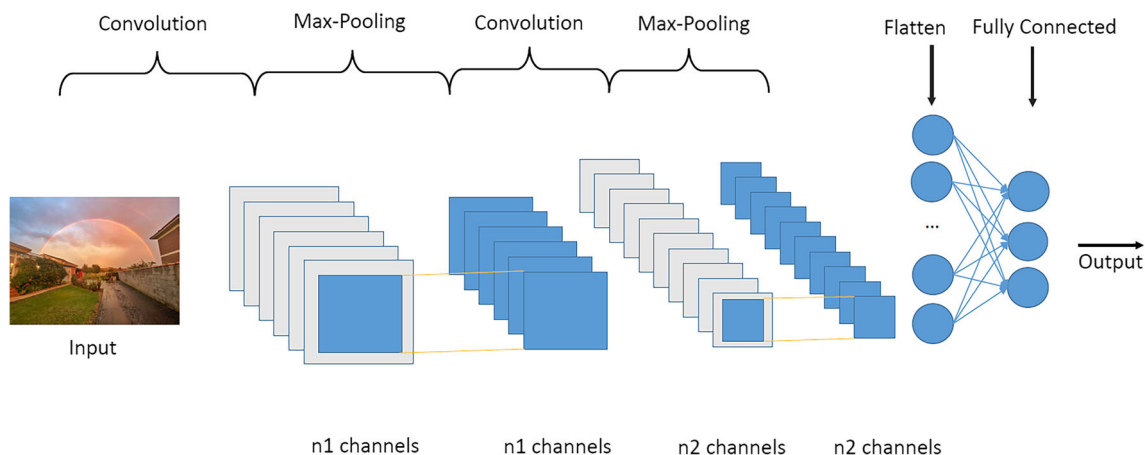


Fig. 5 Vanilla CNN representation

In general, a vanilla CNN has several convolutional layers, and it is also common to add MaxPooling layers to reduce the processing time and one or more fully connected layers to perform classification.

Convolutional layers work with different types of filters, which can change the image by blurring it, using the difference in contrasts to find edges, etc. However, these filters are not configured manually; the convolutional neural network itself is adjusted until it reaches the best performance in regard to recognizing the patterns.

In the CNN training process, the network adjusts the filter weights to produce an accurate feature map for each class.

The scheme of a vanilla CNN is shown in Fig. 5.

4.3 Classical methods

4.3.1 Nearest centroid

This classification model assigns to each new set of input data a descriptor of the photo, in this case, the class of the training data whose centroid is closest to the input data. That is, given a set of labelled samples $(x_1, y_1), \dots, (x_n, y_n)$, where x_i is the data and y_i is the label, this method computes the per-class centroids as represented in (1).

$$\mu = \frac{1}{\|C_l\|} \sum_{i \in C_l} X_i \tag{1}$$

where C_l is the set of indices of the samples belonging to class l . This model assigns to the new input the class: $y = \text{argmin}_{i \in Y} \|\mu_i - x\|$.

4.3.2 Decision trees

A decision tree divides the nodes into all available variables and then selects the division that results in the most homo-

geneous subnodes. The observations are represented by the branches, and the classes are represented by the leaves. A tree is built by splitting the training set, constituting the root node of the tree, into subsets that constitute the successor children. The splitting uses a set of rules based on classification features [53].

4.3.3 Random forest

This method is a combination of predictor trees such that each tree depends on the values of a random vector that is tested independently and has the same distribution for all the trees. It is a substantial modification of bagging that builds a large collection of uncorrelated trees and then averages them [54]. The main idea is that Random Forest builds multiple decision trees and merges them together to obtain a more accurate and stable prediction.

4.3.4 Gaussian naive Bayes

Gaussian naive Bayes is a variant of naive Bayes that follows a Gaussian normal distribution and supports continuous data. The main algorithm is divided into five steps: calculate the prior probabilities for given class labels, create a frequency table with the historical data, calculate the probability for each data point of each class, use the Bayes formula (2) to calculate the posterior probability and finally, assign the class with the highest probability to the input data.

$$P(A_i|B) = \frac{P(B|A_i)P(A_i)}{P(B)} \tag{2}$$

where $P(A_i)$ is the a priori probability, $P(B|A_i)$ is the probability of B conditional on hypothesis A, $P(A_i|B)$ is the posterior probability and $P(B)$ is the probability of observing the evidence.

4.3.5 Local binary pattern

Convolutional networks do not need the image to be described in advance, but in order to use classical machine learning methods and compare our results, the dataset images had to be described, and LBP was used for this purpose.

LBP describes the texture of greyscale images by extracting their local spatial structure with a very low computational cost [55]. For each image pixel, a code is obtained by comparing its value with the value of its neighbours (see (3)):

$$LBP_{P,R} = \sum_{p=0}^{P-1} s(g_p - g_c)2^p \tag{3}$$

$s(x) = 1$ if $x \leq 0$, and $s(x) = 0$ if $x > 0$. g_c is the grey value of the central pixel, g_p is the value of its neighbour p , P is the number of neighbours, and R is the radius of the neighbourhood. The input image is described by creating the histogram of the LBP values at each pixel of the image.

5 Experiments and results

5.1 Experimental setup

First, the dataset captured in the different flights was labelled according to the classes to be recognized. The manual labelling process involved utilizing the entire image for reference. By using the entire image, we can determine the presence of Roman architecture even if it appears in a small or off-centre part of the image, so the experiments are more challenging. After labelling, the data were divided into training and testing sets, as shown in Table 1:

When loading the dataset, a Keras class called ImageDataGenerator was used to avoid collapsing the computer memory when loading batches of 64 images for processing. It was also used to increase the dataset by rotating the images, inverting them horizontally and vertically, and rescaling between 1 and 255 the range of colours that appear in the images, in

Table 1 Dataset split for training and testing with the numbers of images in each class

Class	Train	Test	Total
Channels	1035	611	1646
Crossings	899	518	1417
Mine	998	1084	2082
None	1023	220	1243
	Total		6388

addition to resizing the images to 150 x 150 pixels for faster processing.

For the implementation of the neural network, Keras Python libraries that work on the lowest-level TensorFlow library were used. The CNN is made up of three convolutional and pooling layers to reduce the dimensionality of the feature maps, with a 3x3 kernel in the convolutional layer

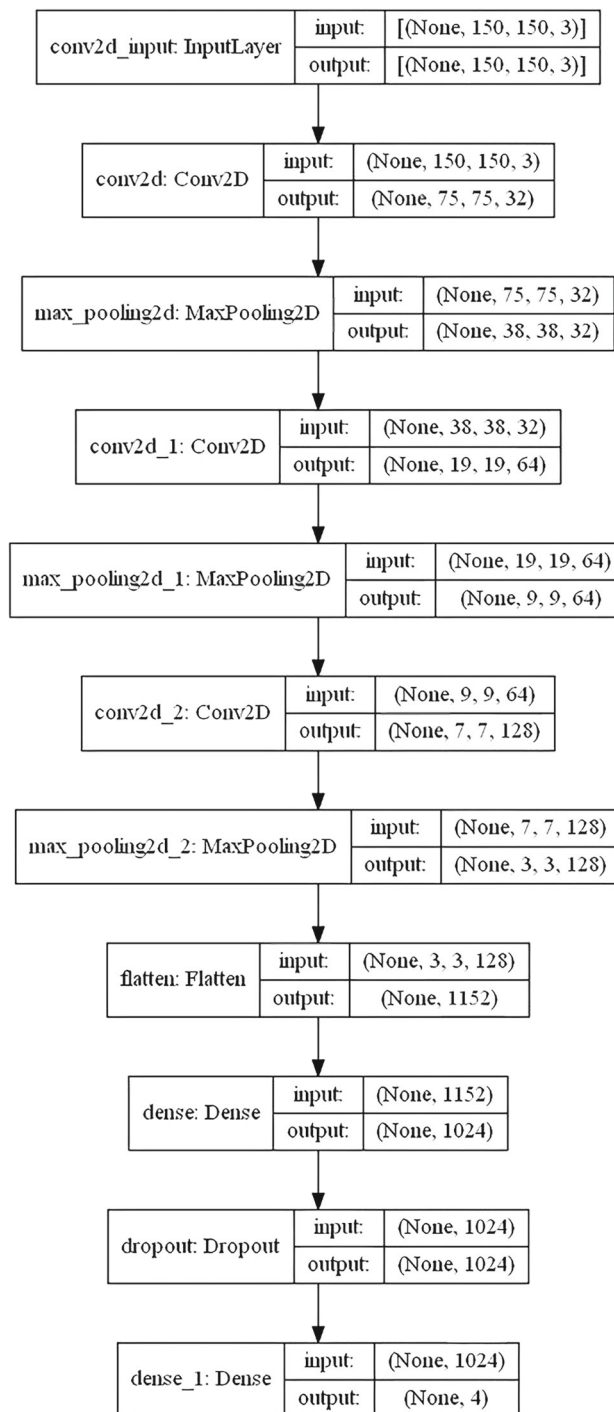


Fig. 6 CNN scheme

and a 2x2 kernel in the reduction layer. After these layers, we reduce the feature maps to just one per image using a Flatten() layer that performs classification. Half of the neurons are deactivated in each iteration by means of dropout layers to avoid overfitting the network, thus making it better able to generalize. The scheme of the CNN is shown in Fig. 6.

5.2 Classification results

The described network was trained for 1000 iterations, and the results were satisfactory, yielding an accuracy of 95.03% over the test dataset. In Fig. 7, it can be seen how the loss function decreases and how the accuracy increases throughout these thousand epochs, demonstrating the good performance of the training process.

To verify the effectiveness of the proposed method, the results were compared with those of other methods, such as Nearest Centroid, Random Forest, decision trees and Gaussian naive Bayes. The advantage of the CNN is that the description and classification processes are carried out at the same time. To evaluate the method with classical classification techniques, it is necessary to make a description of the image first. It was decided to use local binary patterns (LBP), which is one of the best-known image description techniques. Different LBP configurations were tested to verify the classification method in a more robust way. The images were described with LBP 16 (taking into account the 16 nearest neighbours) and LBP 8 (taking into account the 8 nearest neighbours). The results are shown in Table 2.

It can be seen that because convolutional networks can intrinsically describe an image through filters, very promising classification results are obtained in the field, outperforming other classical methods. In terms of classical methods, LBP8 obtained slightly better results than LBP16, with the highest accuracy of 83.48% obtained using Random Forest.

For a better understanding of the performance and limitations of the model, we calculated the confusion matrix

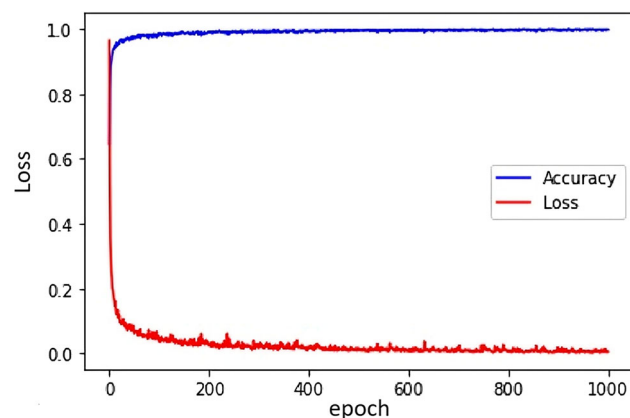


Fig. 7 Evolution of the loss function and accuracy over 1000 epochs

Table 2 Classification results of our proposed CNN compared with classification methods using LBP 8 and LBP 16 as descriptors over the test dataset

	LBP8	LBP 16
Nearest Centroid	0.5902	0.5656
RandomForest	0.8348	0.8282
DecisionTree	0.7678	0.7674
GaussianNB	0.6320	0.6168
CNN	0.9503	

Best result achieved (CNN) is highlighted in the table

for the proposed neural network. These results are shown in Fig. 8. The confusion matrix demonstrates the excellent performance of this model in identifying channels, crossings and mines with 99.18%, 93.82% and 99.17% accuracy, respectively. The greatest imbalance is seen when classifying images without elements, where 34% are classified as crossing. Although this can be improved, the main interest of the experiment is in identifying the elements through UAV images, so these false positives do not affect the objective greatly.

Furthermore, precision, recall and f score were calculated for each of the classes. The results are shown in Table 3.

The outcomes presented herein underscore the commendable performance of the network in effectively discriminating between mines and channels. It is noteworthy that the most suboptimal results are found within the “None” class; however, this discrepancy is inconsequential within the context of the experimental design, which deliberately prioritizes mine detection over potential instances of false negatives, where a mining entity might be present but remains undetected.

6 Discussion

The combination of drones and neural networks has proven to be an extremely versatile tool for identifying elements related to Roman gold mining and differentiating them from other present-day anthropic remains. One of the greatest pitfalls encountered by scientists when identifying mining remains is the degree of subjectivity of their mapping due to various factors [56, 57], both extrinsic (i.e., quality of the images, vegetation, etc.) and intrinsic (i.e., expertise of the mapping technician and digital means available). To overcome this degree of subjectivity, neural networks can help in discriminating digital environments. The mapping of Roman mining remains in NW Iberia presents a high degree of difficulty due to the dense vegetation that covers the mining landscapes and the anthropic modification of the landscape over the last fifty years due to farming practices. A method of reliably discriminating this type of infrastructure can be

Confusion matrix

Predicted	Channel	606 24.91%	1 0.04%	1 0.04%	608 99.87% 0.33%		
	Crossing	5 0.21%	486 19.98%	9 0.37%	74 3.04%	574 84.87% 15.33%	
	Mine			1075 44.18%		1075 100% 0.00%	
	None		31 1.27%		145 5.96%	176 82.39% 17.61%	
	sum_col	611 99.18% 0.82%	518 93.81% 6.18%	1084 99.17% 0.83%	220 65.91% 34.09%	95.03% 4.97%	
		Actual	Channel	Crossing	Mine	None	sum_lin

Fig. 8 Confusion matrix using our proposed CNN

a versatile tool for archaeologists. Furthermore, the identification of characteristic patterns can improve archaeological protection plans, reducing the time needed to analyse and identify these remains, which reduces time-consuming practices and economic resources, especially in a region such as the study region presented in this work, which has more than a thousand kilometres of Roman canals and a large number of mining operations. It is important to highlight that being able to identify ancient mines has enormous potential from a mining point of view, as it facilitates the location of nearby deposits of economic interest, the identification of which has been carried out from the historical analysis of the landscape with the use of LiDAR data, drones and orthoimages [48, 58]. The automatic identification of mining remains has another associated benefit, as mines are often dangerous places where accidents can occur, so administrations must

make an enormous effort to locate and catalogue old mines that have been inactive for years, possibly thousands of years. The latter are the most dangerous, as in many cases, there is no documentation of their presence in the territory. The possibility of identifying pits and ditches can reduce the risk of accidents and can be used for the control and monitoring of current exploitations. The study and control of landslides and subsidence in mining areas has thus far been carried out by remote sensing analysis [59]. However, neural networks could even help in determining the presence of illegal mining in many mining areas, especially in underdeveloped countries where this type of mining is more prevalent [60]. However, remote and automatic detection of features also brings potential benefits for environmental monitoring and can help reduce mining impacts and assist in the administrative control of mining sites, a task that has been carried out

Table 3 Precision, recall and F Score using our proposed CNN for all the different classes evaluated

	Channel	Crossing	Mine	None
Precision	0.997	0.847	1.000	0.824
Recall	0.992	0.938	0.992	0.659
F Score	0.994	0.890	0.996	0.732
Support	611	518	1084	220

to date through image-based surveys [61, 62]. It is also of interest to highlight how the use of drones in recent years has contributed to improving several fields of Roman gold mining archaeology research [58], especially the use of remote sensors, such as multispectral cameras that facilitate the identification of mining remains and hydraulic infrastructure in a fast and effective way [43]. The implementation of these airborne systems for capturing images that are subsequently processed with neural networks can contribute to improving the identification of elements over large and remote areas or difficult-to-access sectors, providing fast and cost-effective results.

In summary, convolutional neural networks (CNNs) have demonstrated exceptional capabilities in image analysis and feature extraction, making them an ideal choice for processing UAV-derived aerial images. These networks leverage convolutional layers to automatically detect hierarchical features such as edges, textures, and patterns within the images. In the context of identifying ancient mining remnants, CNNs excel at recognizing subtle visual cues and variations in terrain, which may not be discernible to the human eye. The mathematical foundation of CNNs, specifically the convolution operation, helps in capturing spatial hierarchies and patterns within the imagery, enabling accurate feature identification.

CNNs not only are powerful in feature extraction but also excel in pattern recognition and classification tasks. The mathematical underpinnings of CNNs, including activation functions and pooling layers, enable the network to learn complex spatial relationships and classify objects with high precision. When applied to UAV-derived images, CNNs can achieve good results by exploiting both the rich spatial information provided by the imagery and the network's inherent ability to learn and generalize from datasets, making them a valuable tool.

This work shows the possibilities of combining new geomatic technologies, such as drones, with neural networks, opening the door to future research aimed at improving the mapping of Roman gold mining remains in NW Iberia. Our methodological approach enhances mapping and man-

agement for archaeologists and mining and environmental companies, as well as administration, which is ultimately responsible for the control, management and preservation of past, present and future mining remains.

7 Conclusions

In this paper, a new method has been proposed to automatically classify Roman gold mining infrastructure from UAV-derived images. We have developed a convolutional neural network architecture that is capable of classifying different common anthropogenic features, such as channels, roads, and mines, with 95.03 % accuracy. The importance of using deep learning is demonstrated by comparing the proposed method with classical image description techniques and conventional classification algorithms. The results show an improvement of 13.39% with respect to the best evaluated classical method, which was Random Forest. The ability of convolutional architectures to identify the best descriptions allows us to obtain much better results than have been obtained to date with other types of techniques. In addition, the use of UAVs for taking images greatly facilitates the capture process and brings this type of solution much closer to the end consumer. These results make it possible to ensure that the identification of Roman infrastructures can be automated, with all that this entails for the related industries.

One promising avenue for future work could involve expanding the scope of the study by incorporating additional mining site locations and significantly augmenting the dataset used for training and validation. By doing so, the method's robustness and predictive power could be enhanced.

Broadening the dataset to encompass a wider range of mining remnants and diverse environmental conditions can lead to a more comprehensive understanding of the model's capabilities. It would enable the algorithm to generalize better across different terrains and mining practices, ultimately making it more powerful in identifying ancient mining remnants from aerial imagery. Future work will involve enabling the user to geolocate targets automatically from coordinates, even in a large area. Furthermore, the inclusion of more locations and data points would help address potential biases and ensure that the model's performance remains consistent and reliable across various scenarios.

Acknowledgements

Funding Open Access funding provided thanks to the CRUE-CSIC agreement with Springer Nature.

Data Availability Statement Data will be made available upon reasonable request.

Computer Code Availability The code used in this paper is called Red-NeuronalTFG and can be found on GitHub under an MIT licence here: https://github.com/dferna10/RedNeuronal_TFG

Declarations

Conflicts of interest All authors declare that they have no conflicts of interest.

Open Access This article is licensed under a Creative Commons Attribution 4.0 International License, which permits use, sharing, adaptation, distribution and reproduction in any medium or format, as long as you give appropriate credit to the original author(s) and the source, provide a link to the Creative Commons licence, and indicate if changes were made. The images or other third party material in this article are included in the article's Creative Commons licence, unless indicated otherwise in a credit line to the material. If material is not included in the article's Creative Commons licence and your intended use is not permitted by statutory regulation or exceeds the permitted use, you will need to obtain permission directly from the copyright holder. To view a copy of this licence, visit <http://creativecommons.org/licenses/by/4.0/>.

References

- Richards-Rissetto H (2017) What can GIS + 3D mean for landscape archaeology? *J Archaeol Sci* 84:10–21. <https://doi.org/10.1016/j.jas.2017.05.005>
- Srivastava PK, Gupta M, Mukherjee S (2012) Mapping spatial distribution of pollutants in groundwater of a tropical area of India using remote sensing and GIS. *Appl Geomatics* 4(1):21–32. <https://doi.org/10.1007/s12518-011-0072-y>
- Chacón J, Irigaray C, Fernández T, El Hamdouni R (2006) Engineering geology maps: landslides and geographical information systems. Springer. <https://doi.org/10.1007/s10064-006-0064-z>
- Pedraza J, Carrasco RM, Villa J, Soteres RL, Karampaglidis T, Fernández-Lozano J, Cirques in the Sierra de Guadarrama and Somosierra Mountains (Iberian Central System): shape, size and controlling factors. *Geomorphology* 341:153–168. <https://doi.org/10.1016/j.geomorph.2019.05.024>
- McMaster RB, Leitner H, Sheppard E (1997) GIS-based environmental equity and risk assessment: methodological problems and prospects. *Cartogr Geogr Inf Sci* 24(3):172–189. <https://doi.org/10.1559/152304097782476933>
- Zollmann S, Schall G, Junghanns S, Reitmayr G (2012) Comprehensible and interactive visualizations of gis data in augmented reality. In: Lecture notes in computer science (including subseries lecture notes in artificial intelligence and lecture notes in bioinformatics), pp 675–685. https://doi.org/10.1007/978-3-642-33179-4_64
- Sermet Y, Demir I (2019) Towards an information centric flood ontology for information management and communication. *Earth Sci Inform* 12(4):541–551. <https://doi.org/10.1007/s12145-019-00398-9>
- Li N, Sun N, Cao C, Hou S, Gong Y (2022) Review on visualization technology in simulation training system for major natural disasters. *Nat Hazards* 112(3):1851–1882. <https://doi.org/10.1007/s11069-022-05277-z>
- Schall G, Zollmann S, Reitmayr G (2013) Smart vidente: advances in mobile augmented reality for interactive visualization of underground infrastructure. *Pers Ubiquit Comput* 17(7):1533–1549. <https://doi.org/10.1007/s00779-012-0599-x>
- Fenais A, Ariaratnam ST, Ayer SK, Smilovsky N (2019) Integrating geographic information systems and augmented reality for mapping underground utilities. *Infrastructures* 4(4). <https://doi.org/10.3390/infrastructures4040060>
- Carrasco RM, Soteres RL, Pedraza J, Fernández-Lozano J, Turu V, Antonio López-Sáez J, Karampaglidis T, Granja-Bruña JL, Muñoz-Martín A (2020) Glacial geomorphology of the high gredos massif: gredos and pinar valleys (Iberian Central System, Spain). *J Maps* 16(2):790–804. <https://doi.org/10.1080/17445647.2020.1833768>
- Woods TL, Reed S, Hsi S, Woods JA, Woods MR (2016) Pilot study using the augmented reality sandbox to teach topographic maps and surficial processes in introductory geology labs. *J Geosci Educ* 64(3):199–214. <https://doi.org/10.5408/15-135.1>
- Suh J, Lee S, Choi Y (2017) Uminear: mobile-tablet-based abandoned mine hazard site investigation support system using augmented reality. *Minerals* 7(10):198. <https://doi.org/10.3390/min7100198>
- Alene GH, Vicari H, Irshad S, Perkis A, Bruland O, Thakur V (2023) Realistic visualization of debris flow type landslides through virtual reality. *Landslides* 20(1):13–23. <https://doi.org/10.1007/s10346-022-01948-x>
- Tian G, Liu J, Yang W (2021) A dual neural network for object detection in UAV images. *Neurocomputing* 443:292–301. <https://doi.org/10.1016/j.neucom.2021.03.016>
- Giordan D, Adams MS, Aicardi I, Alicandro M, Allasia P, Baldo M, De Berardinis P, Dominici D, Godone D, Hobbs P, Lechner V, Niedzielski T, Piras M, Rotilio M, Salvini R, Segor V, Sotier B, Troilo F (2020) The use of unmanned aerial vehicles (uavs) for engineering geology applications. *Bull Eng Geol Environ* 79:3437–3481. <https://doi.org/10.1007/s10064-020-01766-2>
- Fernández-Lozano J, Sanz-Ablanedo E (2021) Unraveling the morphological constraints on roman gold mining hydraulic infrastructure in nw Spain. a UAV-derived photogrammetric and multi-spectral approach. *Remote Sens* 13(2):291. <https://doi.org/10.3390/rs13020291>
- Oscó LP, Junior JM, Ramos APM, de Castro Jorge LA, Fatholahi SN, de Andrade Silva J, Takashi-Matsubara E, Pistori H, Nunes Gonçalves W, Li J (2021) A review on deep learning in UAV remote sensing. *Int J Appl Earth Obs Geoinformation* 102:102456. <https://doi.org/10.1016/j.jag.2021.102456>
- Bonet I, Caraffini F, Peña A, Puerta A, Gongora M (2020) Oil palm detection via deep transfer learning. In: 2020 IEEE congress on evolutionary computation, pp 1–8 (2020, July)
- Bickler SH, Jones B (2021) Scaling up deep learning to identify earthwork sites in the tai tokerau, northland, New Zealand. *Archaeology* 16(1)
- Kokalj Z, Dzeroski S, Sprajc I, Stajdohar J, Draksler A, Somrak M (2023) Machine learning-ready remote sensing data for Maya archaeology. *Sci Data* 10(1):558. <https://doi.org/10.1038/s41597-023-02455-x>
- Kadhim I, Abed FM (2023) A critical review of remote sensing approaches and deep learning techniques in archaeology. *Sensors* 23(6):2918. <https://doi.org/10.3390/s23062918>
- Zhang H, Sun M, Li Q, Liu L, Liu M, Ji Y () An empirical study of multi-scale object detection in high resolution UAV images. *Neurocomputing* 421:173–182. <https://doi.org/10.1016/j.neucom.2020.08.074>
- Török Á, Bögöly G, Somogyi Á, Lovas T (2020) Application of UAV in Topographic Modelling and Structural Geological Mapping of Quarries and Their Surroundings-Delineation of Fault-Bordered Raw Material Reserves. *Sensors* 20(2):489. <https://doi.org/10.3390/s20020489>

25. Fu L, bin Gu W, Li W, Chen L, bao Ai Y, lei Wang H, (2020) Bidirectional parallel multi-branch convolution feature pyramid network for target detection in aerial images of swarm UAVs. *Defence Technology*. <https://doi.org/10.1016/j.dt.2020.09.018>
26. Mittal P, Singh R, Sharma A (2020) Deep learning-based object detection in low-altitude UAV datasets: a survey. Elsevier Ltd. <https://doi.org/10.1016/j.imavis.2020.104046>
27. Tetila EC, Machado BB, Astolfi G, Belete NAdS, Amorim WP, Roel AR, Pistori H (2020) Detection and classification of soybean pests using deep learning with UAV images. *Comput Electron Agric* 179:105836. <https://doi.org/10.1016/j.compag.2020.105836>
28. Peña A, Puerta A, Bonet I, Caraffini F, Gongora M, Ochoa I (2023) A multispectral image classification framework for estimating the operational risk of lethal wilt in oil palm crops. *International conference on the applications of evolutionary computation (Part of EvoStar)*, pp 491–506 (2023, April)
29. Kerkech M, Hafiane A, Canals R (2018) Deep learning approach with colorimetric spaces and vegetation indices for vine diseases detection in UAV images. *Comput Electron Agric* 155:237–243. <https://doi.org/10.1016/j.compag.2018.10.006>
30. Kerkech M, Hafiane A, Canals R (2020) Vine disease detection in UAV multispectral images using optimized image registration and deep learning segmentation approach. *Comput Electron Agric* 174:105446. <https://doi.org/10.1016/j.compag.2020.105446>
31. Zheng H, Zhou X, He J, Yao X, Cheng T, Zhu Y, Cao W, Tian Y (2020) Early season detection of rice plants using RGB, NIR-G-B and multispectral images from unmanned aerial vehicle (UAV). *Comput Electron Agric* 169:105223. <https://doi.org/10.1016/j.compag.2020.105223>
32. Tseng H-H, Yang M-D, Saminathan R, Hsu Y-C, Yang C-Y, Wu D-H (2022) Rice seedling detection in uav images using transfer learning and machine learning. *Remote Sens* 14(12). <https://doi.org/10.3390/rs14122837>
33. Senthilnath J, Dokania A, Kandukuri MKNR, Anand G, Omarkar SN (2016) Detection of tomatoes using spectral-spatial methods in remotely sensed RGB images captured by UAV. *Biosyst Eng* 146:16–32. <https://doi.org/10.1016/j.biosystemseng.2015.12.003>
34. Lan Y, Huang Z, Deng X, Zhu Z, Huang H, Zheng Z, Lian B, Zeng G, Tong Z (2020) Comparison of machine learning methods for citrus greening detection on UAV multispectral images. *Comput Electron Agric* 171:105234. <https://doi.org/10.1016/j.compag.2020.105234>
35. Hossain K, Villebro F, Forchhammer S (2020) UAV image analysis for leakage detection in district heating systems using machine learning. *Pattern Recognit Lett* 140:158–164. <https://doi.org/10.1016/j.patrec.2020.05.024>
36. Lin Y, Jiang M, Yao Y, Zhang L, Lin J (2015) Use of UAV oblique imaging for the detection of individual trees in residential environments. *Urban Forestry and Urban Greening* 14(2):404–412. <https://doi.org/10.1016/j.ufug.2015.03.003>
37. Bu T, Zhu J, Ma T (2022) A uav photography-based detection method for defective road marking. *J Perform Constr Facil* 36(5):04022035. [https://doi.org/10.1061/\(ASCE\)CF.1943-5509.0001748](https://doi.org/10.1061/(ASCE)CF.1943-5509.0001748)
38. Sieberth T, Wackrow R, Chandler JH (2016) Automatic detection of blurred images in UAV image sets. *ISPRS J Photogramm Remote Sens* 122:1–16. <https://doi.org/10.1016/j.isprsjs.2016.09.010>
39. Chen B, Chen Z, Deng L, Duan Y, Zhou J (2016) Building change detection with RGB-D map generated from UAV images. *Neurocomputing* 208:350–364. <https://doi.org/10.1016/j.neucom.2015.11.118>
40. Vasuki Y, Holden EJ, Kovesi P, Micklethwaite S (2014) Semi-automatic mapping of geological structures using UAV-based photogrammetric data: an image analysis approach. *Comput Geosci* 69:22–32. <https://doi.org/10.1016/j.cageo.2014.04.012>
41. Giang TL, Dang KB, Le Toan Q, Nguyen VG, Tong SS, Pham V-M (2020) U-net convolutional networks for mining land cover classification based on high-resolution UAV imagery. *IEEE Access* 8:186257–186273. <https://doi.org/10.1109/access.2020.3030112>
42. Fernández-Lozano J, González-Díez A, Gutiérrez-Alonso G, Carrasco RM, Pedraza J, García-Talegón J, Alonso-Gavilán G, Remondo J, Bonachea J, Morellón M (2018) New perspectives for uav-based modelling the roman gold mining infrastructure in nw spain. *Minerals* 8(11). <https://doi.org/10.3390/min8110518>
43. Fernández-Lozano J, Sanz-Ablanedo E (2021) Unraveling the morphological constraints on roman gold mining hydraulic infrastructure in NW Spain. A UAV-derived photogrammetric and multispectral approach. *Remote Sens* 13(2):291. <https://doi.org/10.3390/RS13020291>
44. Sánchez-Palencia FJ, Fernández-Posse MD, Fernández Manzano J, Orejas A, Pérez LC, Sastre I (2000) Las Médulas (León), un paisaje cultural patrimonio de la humanidad. *Trabajos de Prehistoria* 57(2):195–208. <https://doi.org/10.3989/tp.2000.v57.i2.257>
45. López-Merino L, Peña-Chocarro L, Ruiz-Alonso M, López-Sáez JA, Sánchez-Palencia FJ (2010) Beyond nature: the management of a productive cultural landscape in Las Médulas area (El Bierzo, León, Spain) during pre-Roman and Roman times. *Plant Biosystems* 144(4):909–923. <https://doi.org/10.1080/11263504.2010.491976>
46. Andrés Bercianos F-LJ, Alonso-Gavilán G, Sanz-Ablanedo E. Caracterización de la red de abastecimiento hídrico de la explotación minera de Los Corralones (Espadañedo, Zamora)
47. Ruiz del Árbol M, Sánchez-Palencia FJ (1999) La minería aurífera romana en el Nordeste de Lusitania: las cavenas de El Cabaço (Salamanca). *Archivo Español de Arqueología* 72(179–180):119–139. <https://doi.org/10.3989/aespa.1999.v72.299>
48. Fernández-Lozano J, Gutiérrez-Alonso G, Fernández-Morán MÁ (2015) Using airborne LiDAR sensing technology and aerial orthoimages to unravel roman water supply systems and gold works in NW Spain (Eria valley, León). *J Archaeol Sci* 53:356–373. <https://doi.org/10.1016/J.JAS.2014.11.003>
49. Andrés-Bercianos R, Alonso-Gavilán G, Fernández-Lozano J (2021) Caracterización geológica e identificación de nuevas labores de minería aurífera antigua en los sectores de cabecera de los depósitos tipo raña en el valle del río Negro (Zamora). *Archaeopress*
50. del Árbol Ruiz, Moro M, Sánchez-Palencia Ramos FJ, Sastre Prats I, Saco Orejas, del Valle A (2014) Water networks of Roman gold mines of Northwestern Iberian Peninsula. *Water Hist* 6(1):95–113. <https://doi.org/10.1007/s12685-014-0100-z>
51. Clement Saenz-Ridruejo JVG (1974) Contribucion al estudio de la minería primitiva del oro en el noroeste de España. - Unilibero.com Libros y Coleccionismo. Atlas
52. Fernández-Lozano J, Gutiérrez-Alonso G (2016) Improving archaeological prospection using localized UAVs assisted photogrammetry: an example from the Roman Gold District of the Eria River Valley (NW Spain). *J Archaeol Sci* 5:509–520. <https://doi.org/10.1016/J.JASREP.2016.01.007>
53. Strobl C, Malley J, Tutz G (2009) An introduction to recursive partitioning: rationale, application and characteristics of classification and regression trees, bagging and random forests. *Psychol Methods* 14(4):323. <https://doi.org/10.1037/A0016973>
54. Breiman L, Random Forests. *Machine learning* 45(1):5–32. <https://doi.org/10.1023/A:1010933404324>
55. Ojala T, Pietikäinen M, Mäenpää T. Multiresolution gray scale and rotation invariant texture classification with local binary patterns
56. Lunetta RS, Fenstermaker LK, Lensen JR, Mcgwire KC, Tinny LR, Remote sensing and geographic information system data integration: error sources and research issues
57. Kent RB, Klosterman RE (2007) *GIS and Mapping* 66(2):189–198. <https://doi.org/10.1080/01944360008976098>

58. Currás BX, Javier Sánchez-Palencia F. Landscape archaeology of Roman gold mining in Lusitania: the 'Aurifer Tagus' project. <https://doi.org/10.15184/aqy.2021.82>
59. Perski Z, Hanssen R, Wojcik A, Wojciechowski T (2009) InSAR analyses of terrain deformation near the Wieliczka Salt Mine. Poland. Eng Geol 106(1–2):58–67. <https://doi.org/10.1016/J.ENGGEOL.2009.02.014>
60. Xia Y, Wang Y (2020) InSAR- and PIM-based inclined goaf determination for illegal mining detection. Remote Sens 12(23):3884. <https://doi.org/10.3390/RS12233884>
61. Yang L, Jiuyun S (2011) Study of the integrated environmental monitoring in mining area based on image analysis. Procedia Eng 21:267–272. <https://doi.org/10.1016/j.proeng.2011.11.2014>
62. Padmanaban R, Bhowmik AK, Cabral P (2017) A Remote sensing approach to environmental monitoring in a reclaimed mine area. ISPRS International Journal of Geo-Information 6(12):401. <https://doi.org/10.3390/IJGI6120401>



María Teresa García-Ordás Ph.D. was born in León, Spain, in 1988. She received her degree in Computer Science from the University of León in 2010, and her Ph.D. in Intelligent Systems in 2017. She was a recipient of a special mention award for the best doctoral thesis on digital transformation by TecNALIA. Since 2019, she works at the University of León and since 2023 she works as a full professor in the same institution. Her research interests include computer vision and deep

learning. She has published several articles in impact journals and patents. She has participated in many conferences all over the world.

Publisher's Note Springer Nature remains neutral with regard to jurisdictional claims in published maps and institutional affiliations.



Daniel Fernández-Alonso was born in León, Spain, in 1999. He received his degree in Computer Science from the University of León in 2022, and had a Máster in Artificial Intelligence applied to sports from Catholic University of Murcia in 2023.



Javier Fernández-Lozano holds a Ph.D. in Geological Sciences from the University of Utrecht (The Netherlands). He is a Full Professor and scientist at the Prospecting and Mining Research Area, School of Mines of the University of León. His research is focused on the characterization of gold and iron deposits and mining geomorphology to understand the transformation of ancient mining landscapes, mainly associated with Roman gold mining activity.

He is a UAV pilot and Operator certified by the Spanish Aviation Safety and Security Agency (AESA). He has published in high-impact journals and has participated in several international conferences and workshops worldwide.